

2.4/5.7-GHz Dual-Band Dual-Conversion Low-IF Downconverter Using 0.35 μm SiGe HBT Technology

J.-S. Syu^a, C. C. Meng^a, S.-W. Yu^a, and G.-W. Huang^{b, c}

^a Department of Electrical Engineering, National Chiao Tung University, Hsinchu 300, Taiwan, R.O.C.

^b Department of Electronics Engineering, National Chiao Tung University, Hsinchu 300, Taiwan, R.O.C.

^c National Nano Device Laboratories, Hsinchu 300, Taiwan, R.O.C.

A 2.4/5.7-GHz dual-band dual-conversion low-IF downconverter is demonstrated using 0.35 μm SiGe heterojunction bipolar transistor (HBT) technology. The first image signal is shifted away from the IF band by a complex Weaver architecture while the second image signal is eliminated by a complex Hartley architecture. The downconverter achieves a 45/44-dB image-rejection ratio of the first image (IRR_1) and a 50/48-dB image-rejection ratio of the second image (IRR_2) for 2.4/5.7-GHz modes, respectively, when IF frequency ranges from 20 to 40 MHz.

Introduction

A low-IF receiver is widely used [1]-[3] because this architecture can avoid dc offset and flicker noise problems. Series capacitors can be cascaded at the output to block the dc component in a low-IF receiver while choosing a proper IF band beyond the flicker noise corner can directly escape from the flicker noise problem. In addition, a dual-conversion downconverter alleviates the burden of a high-frequency LO signal generation.

In this paper, a 2.4/5.7-GHz dual-band low-IF downconverter for WLAN 802.11 a/g applications is demonstrated. This work combines the Weaver architecture [4]-[5] and Hartley architecture [6]. The former is a complex dual-conversion system, while the latter consists of a complex mixer and a complex filter, such as a polyphase filter (PPF) [7]-[8] or an active complex band-pass filter [3], [9]-[11].

Circuit Design

Figure 1 shows the block diagram of the 2.4/5.7-GHz dual-band dual-conversion low-IF downconverter consisting of a first-stage single-quadrature complex mixer and a second-stage double-quadrature complex mixer. A single-quadrature complex mixer includes two real mixers with either a quadrature RF or LO input while the other is kept differential. A double-quadrature complex mixer includes four real mixers with both LO and RF signals being quadrature. A Gilbert mixer consists of two current-steering differential amplifiers and thus employing SiGe HBTs in the Gilbert mixer has the advantages of lower LO power and higher conversion gain. A high conversion gain is

helpful to suppress the noise contribution of the following stages, especially the cascaded polyphase filter, to reach a better dynamic range. In addition, Gilbert mixers with output in-phase/anti-phase connections are utilized to realize an addition/subtraction function in the current domain for the complex mixing operation in the second downconversion. The IF buffer amplifier is employed to facilitate 50- Ω measurements.

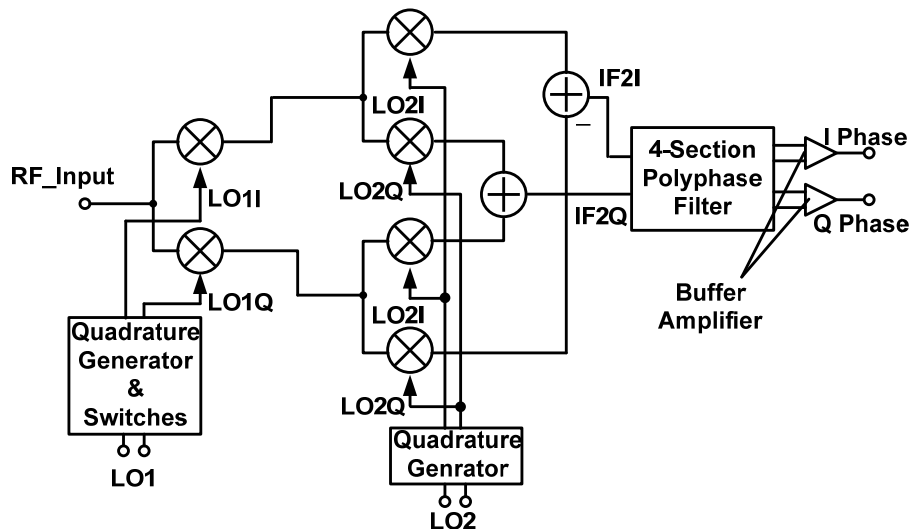


Figure 1. Block diagram of the SiGe HBT 2.4/5.7-GHz dual-band dual-conversion low-IF downconverter.

In this work of a 2.4/5.7-GHz dual-band system, $f_{RFH}=f_{IML}=5.7$ GHz, $f_{RFL}=f_{IMH}=2.4$ GHz. Thus, $f_{LO2}=1.62$ GHz, $f_{LO1}=2.5 \times f_{LO2}=4.05$ GHz, and $f_{IF2}=30$ MHz.

Experimental Result

Figure 4 shows the die photo of the 2.4/5.7-GHz dual-band dual-conversion downconverter and the die size is 1.7×1.4 mm². Figure 5 shows the conversion gain (CG) and the noise figure (NF) of 2.4/5.7-GHz bands with a supply voltage of 3 V. The CG is 11/10 dB and the NF is 19/18 dB for 2.4/5.7-GHz band, respectively, when the IF frequency is below 100 MHz. The downconverter reaches the peak gain when LO₁ power is 13 dBm and LO₂ power is 5 dBm.

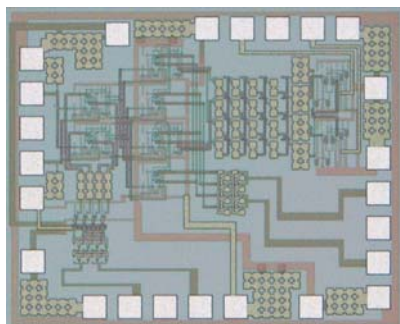


Figure 4. Die photo of the SiGe HBT 2.4/5.7-GHz dual-band dual-conversion low-IF downconverter.

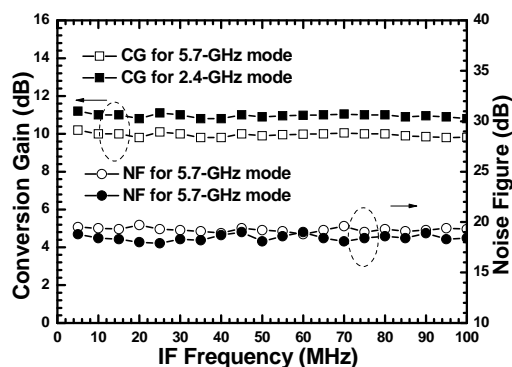


Figure 5. Conversion gain and noise figure of the SiGe HBT 2.4/5.7-GHz dual-band dual-conversion low-IF downconverter.

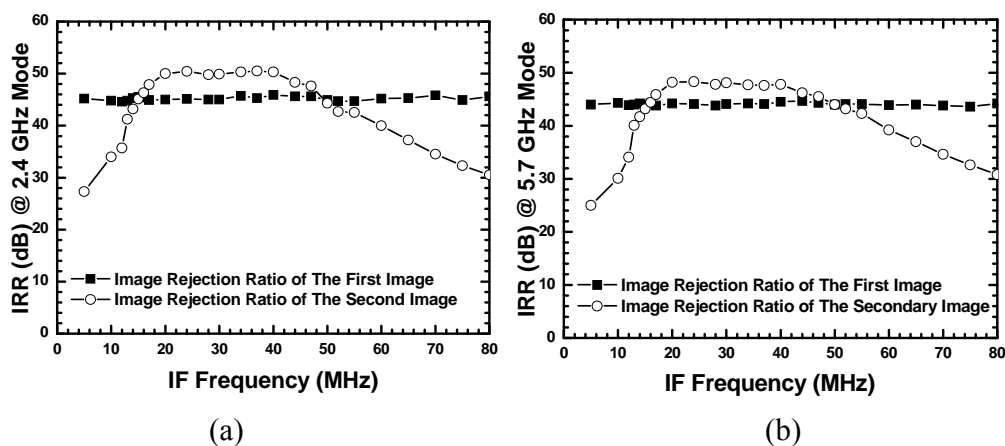


Figure 6. Image rejection ratios of the first/second image signals at (a) 2.4-GHz mode (b) 5.7-GHz mode of the SiGe HBT 2.4/5.7-GHz dual-band dual-conversion low-IF downconverter.

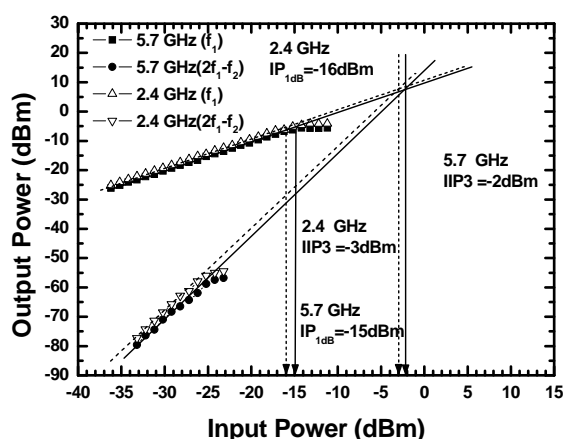


Figure 7. Power performance at 2.4/5.7 GHz mode of the SiGe HBT 2.4/5.7-GHz dual-band dual-conversion low-IF downconverter.

The image-rejection ratios (IRRs) for 2.4/5.7 GHz band are 45/44 dB for the first image and 50/48 dB for the second image as shown in Fig. 6 (a) and (b), respectively. The IRR_1 is flat due to the one-way frequency shifting. Compared with the IRR_1 , the IRR_2 response is a narrow band from 20 to 40 MHz due to the frequency response of the four-section poly-phase filter following the second-stage mixers. Figure 7 shows the power performance of both 2.4/5.7-GHz bands. The IP_{1dB} is -16/-15 dBm and the IIP_3 is -3/-2 dBm for 2.4/5.7-GHz band when $IF=30$ MHz. The output waveforms of both I/Q channels are shown in Fig. 8 and this figure shows a 0.1-dB magnitude mismatch and a 0.7° phase error. Besides, the LO_1/LO_2 -to-RF isolation and the RF-to-IF isolation are shown in Fig. 9(a) and (b), respectively. LO_1/LO_2 -to-RF isolation is better than 65/36 dB while the RF-to-IF isolation is better than 62 dB for both 2.4/5.7-GHz modes. The performance is summarized in Table I.

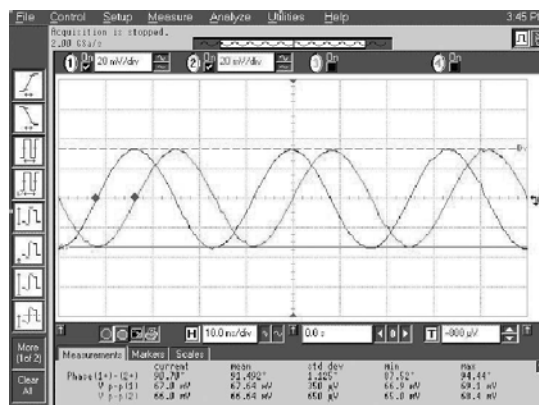


Figure 8. Output I/Q waveforms of the SiGe HBT 2.4/5.7-GHz dual-band dual-conversion low-IF downconverter.

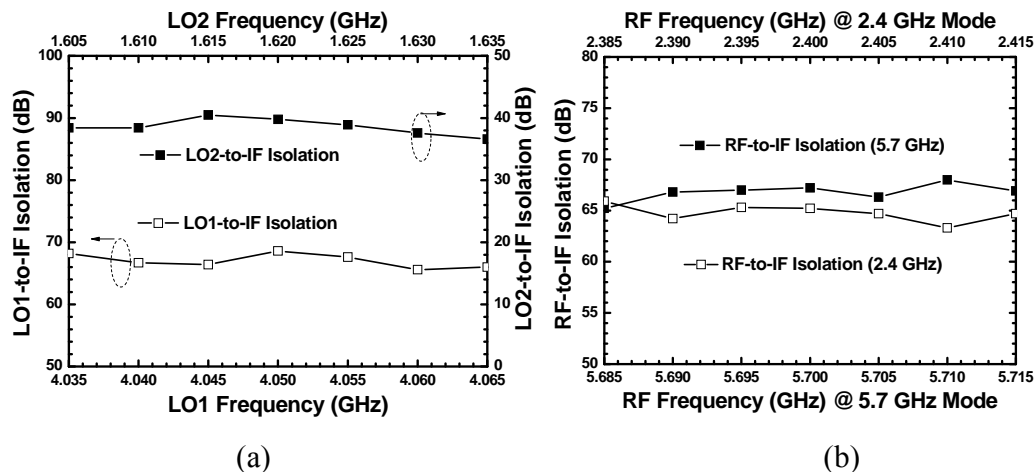


Figure 9. (a) LO_1/LO_2 -to-RF isolation (b) RF-to-IF isolation of the SiGe HBT 2.4/5.7-GHz dual-band dual-conversion low-IF downconverter.

Conclusion

A 2.4/5.7-GHz dual-band dual-conversion low-IF downconverter is demonstrated using $0.35 \mu\text{m}$ SiGe HBT technology. Both differential-quadrature LO_1 and LO_2 signals are generated by a two-section polyphase filter. An 11/10-dB conversion gain and a

19/18-dB noise figure for 2.4/5.7-GHz mode are achieved in this work. Moreover, the IRR_1/IRR_2 are better than 45/50 dB at 2.4-GHz mode while a 44/48-dB IRR_1/IRR_2 is achieved at 5.7-GHz mode when the designed IF band is 20 to 40 MHz.

TABLE I. Performance Summary.

RF Frequency (GHz)	2.4/5.7
LO Frequency (GHz) [f_{LO1}/f_{LO2}]	4.05/1.62
Conversion Gain (dB)	11/10
Single-Sideband Noise Figure (dB)	19/18
Image-Rejection Ratio of the First Image (dB)	45/44
Image-Rejection Ratio of the Second Image (dB)	50/48
IP_{1dB} (dBm)	-16/-15
IIP_3 (dBm)	-3/-2
IF Bandwidth (MHz)	20-40
Supply Voltage (V)	3
Chip Size (mm ²)	1.7×1.4
Technology	0.35- μ m SiGe HBT

Acknowledgments

This work is supported by National Science Council of Taiwan, Republic of China under contract numbers NSC 98-2221-E-009-033-MY3, NSC 98-2221-E-009-031 and NSC 98-2218-E-009-008-MY3, NSC 98-2120-M-009-010, and by MoE ATU Program under contract number 95W803. The authors would like to thank National Chip Implementation Center (CIC) for technical support.

References

1. S. J. Fang, A. Bellaouar, S. T. Lee, and D. J. Allstot, *IEEE Trans. Microw. Theory Tech.*, **53**(2), 478 (2005).
2. W. Kluge, F. Poegel, H. Roller, M. Lange, T. Ferchland, L. Dathe, and D. Eggert, *IEEE J. Solid-State Circuits*, **41**(12), 2767 (2006).
3. I. Nam, K. Choi, J. Lee, H.-K. Cha, B.-I. Seo, K. Kwon, and K. Lee, *IEEE Trans. Microw. Theory Tech.*, **55**(4), 682 (2007).
4. D. Weaver, *Proceedings of the IRE*, 1703 (1956).
5. T.-H. Wu and C. C. Meng, *IEEE J. Solid-State Circuits*, **41**(11), 2468 (2006).
6. R. Hartley, U.S. Patent 1,666,206, (1928).
7. F. Behbahani, Y. Kishigami, J. Leete, and A. A. Abidi, *IEEE J. Solid-State Circuits*, **36**(6), 873 (2001).
8. F. Behbahani, J. C. Leete, Y. Kishigami, A. Roithmeier, K. Hoshino, and A. A. Abidi, *IEEE J. Solid-State Circuits*, **35**(12), 1908 (2000).
9. J. Crols and M. Steyaert, *IEEE J. Solid-State Circuits*, **30**(12), 1483 (1995).
10. S. Tadjpour, E. Cijvat, E. Hegazi, and A. A. Abidi, *IEEE J. Solid-State Circuits*, **36**(12), 1992 (2001).
11. C. C. Meng, T.-H. Wu, J.-S. Syu, S.-W. Yu, K.-C. Tsung, and Y.-H. Teng, *IEEE Trans. Microw. Theory Tech.*, **57**(3), 552 (2009).